The role of post-translational modifications by ubiquitin/ISG15 tags in exposed proteins during NETosis: Immunogenic or tolerogenic signaling process in Systemic Lupus Erythematosus?

Daniel Alberto Carrillo-Vázquez

Department of Internal Medicine. Instituto Nacional de Ciencias Medicas y Nutricion Salvador Zubiran. Department of Immunology and Rheumatology. Instituto Nacional de Ciencias Médicas y Nutrición Salvador Zubirán, Mexico City, Mexico Department of Immuno https://orcid.org/0000-0002-9417-8867

Eduardo Jardón-Valadez.

Earth Resources Department, Universidad Autónoma Metropolitana. Lerma, Estado de Mexico 52005, Mexico.

Jiram Torres-Ruiz

Emergency Medicine Department. Instituto Nacional de Ciencias Médicas y Nutrición Salvador Zubirán, Mexico City, Mexico. Department of Immunology and Rheumatology. Instituto Nacional de Ciencias Médicas y Nutrición Salvador Zubirán, Mexico City, Mexico

Guillermo Juárez-Vega

Red de Apoyo a la Investigación. Coordinación de Investigación Científica, Universidad Nacional Autónoma de México, Mexico City, Mexico

José Luis Maravillas-Montero

Red de Apoyo a la Investigación. Coordinación de Investigación Científica, Universidad Nacional Autónoma de México, Mexico City, Mexico

David Eduardo Meza-Sánchez

Red de Apoyo a la Investigación. Coordinación de Investigación Científica, Universidad Nacional Autónoma de México, Mexico City, Mexico

María Lilia Domínguez-López

Department of Immunology. Escuela Nacional de Ciencias Biológicas, Instituto Politécnico Nacional, Ciudad de México, México

Jorge Carlos Alcocer Varela

Department of Immunology and Rheumatology. Instituto Nacional de Ciencias Médicas y Nutrición Salvador Zubirán, Mexico City, Mexico

Diana Gomez-Martin (d_gomar@hotmail.com)

Department of Immunology and Rheumatology. Instituto Nacional de Ciencias Médicas y Nutrición Salvador Zubirán, Mexico City, Mexico. Red de Apoyo a la Investigación. Coordinación de Investigación Científica, Universidad Nacional Autónoma de México, Mexico https://orcid.org/0000-0002-1807-0045

Research

Keywords: NETs, post-translational modifications, myeloperoxidase, ubiquitin, ISG15, Lupus

Posted Date: July 24th, 2020

DOI: https://doi.org/10.21203/rs.3.rs-44910/v1

Version of Record: A version of this preprint was published on November 11th, 2020. See the published version at https://doi.org/10.1186/s12967-020-02604-5.

Abstract

Background: Neutrophil extracellular traps (NETs) from patients with Systemic Lupus Erythematosus (SLE) are characterized by lower ubiquitylation and myeloperoxidase (MPO) as a substrate. The structural and functional effect of such modification and if there are additional post-translational modifications (PTMs) are unknown.

Methods: To assess the expression and functional role of PTMs in NETs of patients with SLE; reactivation, proliferation and cytokine production was evaluated by flow cytometry using co-cultures with dendritic cells (DC) and $CD4^+$ from SLE patients and healthy controls. The impact of ubiquitylation on MPO was assessed by molecular dynamics. The expression of ISG15 in NETs was evaluated by immunofluorescence and Western Blot.

Results: Fifteen patients with SLE and 10 healthy controls were included. In the co-cultures of $CD4^+$ lymphocytes with DC stimulated with ubiquitylated MPO or recombinant MPO, a higher expression of IFNγ and IL17A was found in $CD4^+$ from SLE patients ($p < 0.05$). Furthermore, with DC stimulated with ubiquitylated MPO a trend towards increased expression of CD25 and Ki67 was found in lupus $CD4^+$ lymphocytes, while the opposite was documented in controls ($p < 0.05$). Through molecular dynamics we found the K129-K488-K505 residues of MPO as susceptible to ubiquitylation. Ubiquitylation affects the hydration status of the HEME group depending on the residue to which it is conjugated. R239 was found near by the HEME group when the ubiquitin was in K488-K505. In addition, we found greater expression of ISG15 in the SLE NETs vs controls ($p < 0.05$), colocalization with H2B ($r = 0.78$) only in SLE samples and increased production of IFNγ in PBMCs stimulated with lupus NETs compared to healthy controls NETs.

Conclusion: The ubiquitylated MPO has a differential effect on the induction of reactivation and proliferation of $CD4^+$ lymphocytes in patients with SLE, which may be related to structural changes by ubiquitylation at the catalytic site of MPO. Besides a lower ubiquitylation pattern, NETs of patients with SLE are characterized by the expression of H2B conjugated with ISG15, and the induction of IFNγ by Th1 cells.

Introduction

Neutrophil extracellular traps (NETs) play a pathogenic role in diverse autoimmune diseases, including systemic lupus erythematosus (SLE) (1). These NETs are fibrillar mesh structures decorated by nuclear chromatin and neutrophil granular peptides (i.e. myeloperoxidase, elastase, lactoferrin and LL-37) and are one of the most potent tools to combat microorganisms(2). Likewise, these structures are a potential source of autoantigens, whose externalization might lead to self-tolerance breakdown. Indeed, enhanced NETosis, diminished clearance or posttranslational modifications in the protein cargo of these NETs are related to tissue damage in SLE (3). Diverse stimuli have been acknowledged, including those related to microorganisms, such as LPS, inflammatory stimuli (ie ROS, TNF-α and IL-8) as well as those considered

as sterile, such as the antigen-antibody complexes (4). Indeed, Petretto A, *et al* (4) showed by proteomic analysis a differential protein cargo and post-translational modifications, dependent upon the induction stimuli for NETosis, Interestingly the majority of modified peptides are derived from myeloperoxidase (MPO), which might be responsible for diverse biologic effects (4). This enzyme catalyzes the transformation of hydrogen peroxide in hypochlorous acid, hence MPO has a bactericidal function. MPO is key for the NETosis induction, since it acts synergistically with neutrophil elastase (NE) for the degradation of membranes and chromatin decondensation (5). Furthermore, MPO has been acknowledged as a dual modulator of immune responses, particularly when it is located at the extracellular milieu, where it is able to induce tissue damage mediated by increased oxidative stress (6). At the cellular level, MPO induces T cell proliferation in a dose dependent manner in antineutrophil cytoplasmic antibodies (ANCA) associated vasculitis and healthy donors (7), as well as having an immunosuppressive role, mediated by IL-10 (8) and by dendritic cell suppression through reduced CD86 and IL12 expression (6).

Post-translational modifications (PTMs) have been related to NETosis induction and its pathogenic role in autoimmune diseases has been acknowledged, since it implies a mechanism for neoantigen expression. Indeed, citrullination of histone 2B during NETosis is a key element for pathogenic autoantibody responses in SLE (9). Furthermore, NETs from SLE patients are characterized by a differential PTM profile, including histone hyperacetylation (10) and a deficient polyubiquitilation (K48/K63) profile (11), which induce pro-inflammatory macrophage responses. Among PTMs with potential regulatory role in autoimmune pathogenic responses, the ISGylation, defined as the conjugation of the ubiquitin-like-protein ISG15; is related to enhanced type I IFN responses (12) besides that, extracellular ISG15 also promotes the synthesis of IFNγ by T and B cells. Additionally, NETs are potent inducers of IFNα/β by plasmacytoid dendritic cells in SLE (13) and type I IFN responses are the hallmark of the molecular signature in SLE. Nonetheless, it has not been addressed if ISGylation is present in NETs from SLE patients as a potential source of ISG15 and a regulator of IFN responses.

Evidence suggests that PTMs, particularly ubiquitylation and ISGylation might play a role for enhanced NETosis in SLE and particularly, MPO was shown to be target of this PTM in NETs from SLE patients and healthy donors (11). However, the precise amino acid residue where ubiquitin tag is added is currently unknown, as well as its potential impact in cellular responses. Therefore, the aim of the present work is to address the role of PTMs related to ubiquitin and ubiquitin-like-protein, ISG15 from NETs and their effects in the regulation of cellular responses in SLE.

Materials And Methods

Patients and controls. We recruited 15 Mexican-mestizo adult patients with active SLE (SLEDAI > 6) according to the ACR criteria (14), who were followed-up in a tertiary care center (Instituto Nacional de Ciencias Médicas y Nutrición Salvador Zubirán). As a control group, ten age and gender matched healthy subjects were included. Exclusion criteria were applied to those patients with any kind of acute or chronic infection, pregnancy, puerperium and neoplasia. All healthy controls and SLE patients signed an informed

consent before inclusion, and the protocol was approved by our Institutional Ethics Committee (Ref. 2152) in compliance with the Helsinki declaration. Laboratory features of SLE patients were assessed as follows: *Auto* antibodies of SLE patients (anti-dsDNA IgG, anti-nucleaosomes, anti-cardiolipin and anti-β2glycoprotein I) were assayed using a commercial ELISA.

In vitro ubiquitylation of MPO. A commercial *Ubiquitylation Kit (Abcam™)* (HeLa lysate) was used according to the manufacturer's instructions. The recombinant human MPO (rhMPO 10 µg) was incubated for 4 h at 37 ° in a water bath and stored at -80°. To confirm that the ubiquitylation reaction took place, a 4–15% polyacrylamide gel electrophoresis was performed with 50 µg of ubiquitylated MPO (UbMPO) and rhMPO. Subsequently, the transfer to a PVDF membrane was carried out for 1 h at 100v, then, the non-specific binding sites were blocked with Starting Block solution (*Thermo Fisher ™*). Overnight incubation was carried out with the primary anti-ubiquitin antibody (P4D1 *Santa Cruz™*) and followed by the secondary antibody HRP anti-Mouse for 1 h (*Thermo Fisher™*). Membranes were developed by enhanced chemiluminiscence with ECL Western Blotting Substrate (*BioRad™*). Samples were acquired with a digital image analyzer (*Chemidoc MP™, Biorad™*) and quantified by densitometry with ImageLab software (*Biorad™*). (Figure S1).

T cell responses upon ubiquitylated MPO (UbMPO). To address T cell responses, cocultures of mature in vitro $CD4^+$ T lymphocytes and monocyte derived dendritic cells (MoDCs) were set up and stimulated with either the native MPO (recombinant human MPO, rhMPO) (5 µg/ml) or UbMPO (5 µg/ml).

Monocyte isolation and MoDCs generation: Peripheral blood mononuclear cells (PBMCs) were isolated from SLE patients and healthy controls by density gradients after centrifugation with *Ficoll-Paque PLUS (GE Healthcare™*). After washing twice with 5% fetal bovine serum (FBS) in PBS, PBMCs were resuspended in RPMI 1640 medium (*Gibco™*) supplemented with 10% FBS and 100,000 cells were incubated for 30 min at 4 °C in MACS buffer and anti-CD14 antibodies from CD14 MicroBeads Isolation Kit conjugated with magnetic beads (*Miltenyi Biotec ™*) to obtain the enriched $CD14^+$ population. To induce differentiation to dendritic cells, GM-CSF (*R&D™*) (50 ng/ml) and IL4 (*PeProTech™*) (30 ng/ml) were added. $CD14^+$ monocytes were seeded in 6-well plates in 4 ml (1×10^6 per ml of medium). On the third day, medium change was performed (15). After seven days, DCs were harvested and viability was evaluated using the trypan blue method. They were seeded in 24-well plates (1×10^6 cells per ml of medium). Cells were divided into three reactivation conditions for 24 h (16): a) LPS (1 µg/ml) E. coli O111: B4 LPS (*Sigma Aldrich™)*; b) LPS (1 µg/ml) and rhMPO R&D™ (5 µg/ml); and c) LPS (1 µg/ml) and ubiquitylated MPO (5 µg/ml).

$CD4^+$ T cell isolation and $CD4^+$/MoDC cocultures: Both lupus and control $CD4^+$ T cells were also isolated from total PBMCs by magnetic negative selection with microbeads according to the Human $CD4^+$ Isolation Kit manufacturer instructions (*Miltenyi Biotec™)*. $CD4^+$/MoDC cocultures were performed in a 10:1 ratio at 37 °C, and 4% CO_2 for 3 days to evaluate proliferation and for 7 days to evaluate reactivation and cytokine production from $CD4^+$ T cells. The cocultures were set up as follows: a) Unstimulated $CD4^+$

cells; b)$CD4^+$ cells plus DCs activated only with LPS; c) $CD4^+$ cells plus DCs activated with LPS and rhMPO; d)$CD4^+$ cells plus DCs activated with LPS and ubiquitylated MPO; and e)$CD4^+$ cells polyclonally stimulated with 50 ng/mL of αCD3 *(HIT3a BD™)* and 100 ng/mL of αCD28 (*NA/LE BD™).*

$CD4^+$ T cell proliferation and activation markers assessment by flow cytometry: For the assessment of activation markers, after washing twice with 5% FBS in PBS and incubated with FVS700 to evaluate viability, PBMCs were stained with the following fluorescent surface labelled-antibodies: (CD4-APC, CD25-PE, CD83-PE/Cy5, HLA-DR-PerCP) *(*All *Bio Legend™)*. After that, the cells were fixed with *True-Nuclear™ 1X Fix Concentrate*, then washed with *FoxP3-Perm Buffer™* and finally incubated with labelled anti-FoxP3 BV421. For the proliferation assay, the same steps described above were performed and after fixation and permeabilization, PBMCs were incubated with anti Ki67-APC *(Bio Legend™)* instead.

For intracellular cytokine staining, PBMCs were stimulated with PMA (*Sigma™)*, ionomycin from *Streptomyces conglobatus (Sigma™)* and incubated with monensin *(GolgiStop™, BD Horizon™)* at 37ºC for 5 h. After washing twice with 5% FBS in PBS, PBMCs were stained with anti CD4-AF488 and then fixed and permeabilized with *Cytofix/cytoperm (BD™)*, and finally incubated with intracellular anti IFNγ-APC (Th1), IL4-PE (Th2), IL17A-BV421V (Th17) (*Bio Legend™)* (Figure S2).

Molecular Dynamics Methods. To assess the initial positions of all-atoms of the backbone of the MPO were taken from the cryogenic crystal structure isoform C, PDB:1CXP, chains A and C (17), while the ubiquitin coordinates were taken from the crystal structure, PDB:1UBQ, chain B (18). To approach the post-translational modifications of MPO, the solvent accessible surface area (SASA) and the root mean square deviation (RMSD) fit of MPO at lysine residues with K6, K48 and K63 of the ubiquitin, were used as criterium to identify exposed lysines. Larger values of SASA were used to identify susceptible residues for ubiquitylation (an enzymatic reaction that its defined by an isopeptide bond among the amino group of substrate lysine chains and the carboxyl terminus G63 of ubiquitin).

To the generation of simulation trajectories, MPO was defined as the center in the simulation box and the water molecules were added via the solvate plugin of VMD 1.9.1 program (19), filling the space around the protein after a 2 Å cutoff. To define the physiologic electrolyte concentration of NaCl at 0.15 M we used the ionized VMD plugin (19). Every system was committed to energy minimization for 10 K steps of conjugate gradient algorithm. Later, the crystallographic structure was relaxed in steps of 200 ps each, with positional constraints setting force constants of 25, 15, 10 5 3, 2 ,1 kcal/mol Å. After pre-equilibration, all simulation trajectories were produced with the NAMD 2.12 program (20). Configurations in the isothermal-isobaric ensemble, at 300K and 1 bar conditions, were generated using Langevin dynamics scheme to maintain constant temperature (20), and a Nose-Hoover Langevin piston for pressure control (21, 22). For computational efficiency, a multiple time-step integration scheme was set, with 1 fs for bond forces, 2 fs for short-range non-bonding interactions, and 4 fs for full electrostatic forces (23, 24). Coulomb interactions were computed using particle-mesh smooth Ewald summation (25, 26) with a tolerance of 10^{-6} for the direct part of the Ewald sum, a fourth-order interpolation scheme, and a grid spacing of ~ 1 Å, for each direction of the simulation box. All bonds for hydrogen atoms were

constrained using the SHAKE algorithm (27). All-atom force field parameters were used in this study. The CHARMM 36 force field (28–30) with CMAP correction for the protein atoms (31), and the TIP3P water model (32). In house analysis scripts were developed for specific calculations, such as hydration level at the active site, heme group contact maps.

ISG15 detection in ex vivo NETs by Western Blot. After density gradients, neutrophils were isolated with dextran sedimentation as previously described (33). We assessed the spontaneous NET formation (without stimuli) and lipopolysaccharide (LPS)-induced NETosis with 1 µg/mL E. coli O111:B4 LPS (*Sigma Aldrich* ™) for 4 h. Subsequently, 300 µL of RPMI with micrococcal nuclease (0.01U/µL) were added, the supernatant was centrifuged and stored at -20 °C. The protein was quantified using the bicinchoninic acid method at a wavelength of 562 nm. 4–15% polyacrylamide gel electrophoresis was performed on the lysates from the NETs of patients with SLE and healthy controls. Subsequently, the transfer was carried out for one hour at 100v to a PVDF membrane. Nonspecific binding sites were blocked with the Starting Block *Thermo Fisher*™ solution. The membrane was then incubated overnight with anti-ISG15 (*Abcam* ™), after 3 washes with TBS-tween, the secondary antibody HRP anti-Rabbit (*Thermo Fisher™*) was added for 1 h. Membranes were developed by enhanced chemiluminiscence with ECL Western Blotting Substrate (*BioRad).* Samples were acquired with a digital image analyzer (*Chemidoc MP, Biorad*) and quantified by densitometry with *ImageLab* software (*Biorad*). Data was expressed as normalized expression to MPO.

Assessment of ISG15 in ex vivo NETs by confocal microscopy. Neutrophils were incubated in RPMI without phenol red (*Thermo Fisher* ™), 1% FBS, and 1% 10 mM 4-(2-hydroxyethyl)-1-piperazineethanesulfonic acid (HEPES) buffer. For confocal microscopy, neutrophils were seeded in 0.01% poly-L-Lysine (*Sigma-Aldrich ™*) coated coverslips at 37ºC during 1.5 h. After fixation with 4% paraformaldehyde (*Santa Cruz ™*) (33) at 4ºC during 24 h, washing and blocking with 0.2% gelatin from porcine skin (*Sigma-Aldrich* ™) was performed. For indirect immunofluorescence, we used the following primary and secondary antibodies diluted in 0.2% gelatin from porcine skin: rabbit anti-human ISG15 (*Abcam™*), mouse anti-human H2B (*Abcam™*), donkey anti-rabbit Alexa Fluor 555 (*Thermo Fisher™*) and donkey anti-mouse Alexa Fluor 488 (*Thermo Fisher™*). Chromatin was stained with Hoechst 33342 (*Thermo Fisher™*) and coverslips were mounted on slides with ProLong® Gold Antifade Mountant (*Thermo Fisher™*)(34). The samples were acquired in an Eclipse Ti-E Nikon confocal microscope (Minato, Tokyo, Japan). The number of cells positive for H2B and nuclear staining (Hoechst) were considered producers of NETs. The mean fluorescence intensity and the area percentage of NETs were quantified using Fiji free software (*ImageJ* ™) using the average of 6 fields at 40x, normalized for the total number of cells analyzed. The colocalization of ISG15 with histone 2B (H2B) was calculated by Pearson correlation coefficient and validated through the Costes method (35).

Flow cytometry assessment of IFNγ production in PBMC's stimulated with NETs enriched in ISG15. To evaluate IFNγ production, 2×10^6 healthy donor's PBMCs were stimulated with 100 µg/mL of SLE NETs enriched in ISG15, and NETs from healthy controls lacking ISG15 (expression of ISG15 were corroborated by Western Blot and immunofluorescence, as previously described) or PMA *Sigma*™ (50 ng/mL) and

ionomycin from *Streptomyces conglobatus Sigma*™ (1 µg/mL) as a positive control. Monensin (*GolgiStop*™ *BD Horizon*™) were added and incubated at 37ºC for 18 h. After washing twice with 5% FBS in PBS, PBMCs were stained with the following fluorescent surface labelled-antibodies: (CD3-APCH7, CD4-AF488, CD8-PE/Dazzle, CD56-PE, CD335-BV711) (All *Bio Legend™)*. $CD4^+$ cells were defined as $CD3^+CD4^+$, $CD8^+$ cells were $CD3^+CD8^+$ and NK cells were $CD3^-CD56^+CD335^+$. After that, the cells were fixed and permeabilized with *Cytofix/cytoperm BD™*, and finally incubated with intracellular anti IFNγ-APC (Th1) (*Bio Legend™).* The samples were acquired on a *BD LSRFortessa* flow cytometer. Data analysis was performed with the support of *FlowJo* 10.6 software (*FlowStar Inc ™).*

Statistical analysis. Quantitative variables were expressed as median with interquartile range (IQR) or minimum and maximum (min-max). The homogeneity of variances of each experiment was determined using the Brown-Forsythe and Bartlett tests. The non-parametric data were analyzed with the Kruskall-Wallis test and the adjustment was made using the Dunn multiple comparison test, as well as Mann-Whitney U test (sum of Wilcoxon ranges) to compare medians between groups with free software *Past 3* version™ (United States). Pearson's linear correlation coefficient was used (36), and significance was verified using the Costes method (35). In all cases, significant differences were considered fora p value lower than 0.05. Statistical analysis and graph generation was performed with support of the *GraphPad Prism 8* version ™ software (United States).

Results

Demographic and clinical features of patients with SLE. Table 1 shows the main characteristics of the fifteen patients with active SLE included (SLEDAI > 6), of which 80% were women and 20% men. The median age was 27.18 years (19–35 years). The disease activity was measured using the SLEDAI score (37) with a median of 20 points (8–24), 90.0% had constitutional activity, 82% renal activity, 72.7% hematological activity and 63.6% mucocutaneous activity at the time of the blood draw. All had positive anti-nuclear antibodies in different patterns, 86.6% had anti-dsDNA IgG in positive titers with a median of 142 IU/mL (2.1–485 IU/mL), 33.3% had anti- nucleosomes with a median of 209 U/mL (11.4–660 U/mL). 86% of patients had hypocomplementemia. All patients used immunosuppressive treatment at the time of sampling.

Table 1
Clinical and laboratory features of patients with SLE (n = 15)

Variable	Median (IQR)
Disease activity	
SLEDAI	20 (8–24)
General laboratory features	
Total leukocyte count (x 10^9 x L)	5.087 (4-10.1)
Total neutrophil count (x 10^6 x L)	5087 (3266–7979)
Total lymphocyte count (x 10^6 x L)	1390 (846–1847)
Neutrophil / lymphocyte index	8 (1–19)
Hemoglobin (g / dL)	10.5 (6.6–13.7)
Creatinine (mg / dL)	1.8 (0.6–5.19)
C3 (mg / dL)	57 (32–110)
C4 (mg / dL)	8 (8–28)
Proteinuria (mg/24 h)	7555.3 (1866–19564)
Proteinuria-Creatinuria Index (CPI) g/g	5.78 (1.5–14.5)
Immunological tests	
anti-DNAdc IgG (ELISA-FARR) (IU / mL)	141.1 (2.1–658)
anti-Nucleosomes (U / mL)	209 (11.4-659.7)
IgM anti-cardiolipin (UMPL)	10.9 (7.3–33.8)
anti-cardiolipin IgG (UGPL)	8.95 (4.7–65.3)
anti-β2glycoprotein I IgM (U / mL)	4.3 (3-14.2)
anti-β2glycoprotein I IgG (U / mL)	4.05 (2.8–72.5)
Positive Lupus anticoagulant	20%
Immunosuppressive Therapy	
Prednisone dose (mg / day)	51.8 (10–70)
Azathioprine dose (mg / day)	1.25 (1.25–1.25)
Mycophenolic acid dose (gr / day)	3 (2.5-3)
Cyclophosphamide dose (gr / month)	1 (0.8–1.4)

Variable	Median (IQR)
Dose of hydroxychloroquine (mg / day)	200 (150–400)

UbMPO induces a differential proliferation and activation profile as well IFNγ and IL17A production. By means of intracellular cytokine staining, increased production of IFNγ (Panel A Fig. 1) and IL17A (Panel B Fig. 1) was found in SLE $CD4^+$ T lymphocytes co-cultured with dendritic cells activated with rhMPO and UbMPO compared to the group in which the co-culture included DC activated only with LPS ($p = 0.0286$). In SLE patients, a trend towards increased proliferation was observed only in the $CD4^+$ lymphocytes stimulated with UbMPO/LPS in comparison with both, the lymphocytes activated with rhMPO/LPS (UbMPO/LPS vs rhMPO/LPS $p = 0.1143$) and with those activated with LPS in the absence of MPO (UbMPO/LPS vs LPS $p = 0.1143$) (Panel C Fig. 1).

Additionally, stimulation with UbMPO was associated to lower expression of CD25 in $CD4^+$ lymphocytes from healthy controls, compared to those T cells cocultured with dendritic cells activated only with rhMPO (UbMPO MFI [1751(1308–1889)] vs rhMPO MFI [2127(2042–2501] $p = 0.0286$ (Panel D Fig. 1). Likewise, a lower proliferation (Ki67 expression) was evidenced in $CD4^+$ T lymphocytes from healthy donors that were cocultured with dendritic cells stimulated with UbMPO compared to those activated with rhMPO. (UbMPO% [9.93 (8-10.3)] vs rhMPO% [11(10.5-11.73)] $p = 0.0421$), (Panel E Fig. 1) (Supplementary Table 1).

Ubiquitylation of MPO is related to HEME group modifications: The HEME group was attached to D94 of chain α, and E242 of chain β, using an ester bond among methyl groups of catalytic site and carboxyl side chains of the subunits (Panel A Fig. 2). Also, owed to its proximity to the HEME active site, the D98 was protonated, as suggested by Carpena, *et al* (38). We found three lysine: (K129-MPO, K488-MPO, and K505-MPO) as the best candidates for ubiquitylation and prepared four systems for detecting structural and conformational changes made by ubiquitylation (Panel B Fig. 2). *Contact Maps at the active site.* Through the analysis of relative frequencies in the contact map of the residues close to the HEME group, with a cutoff point for bond distance < 2 Å (Panel C of Fig. 2); differential profiles were found depending on the ubiquitin binding site to the MPO. In this way, R239 was found near the HEME group when ubiquitin was at positions K505 or K488 (Panel D Fig. 2).

Hydration of the active site. To investigate the dynamics of the water molecules in the active site, we measure the number of water molecules at 3 Å from the HEME group. Interestingly, ubiquitylation seemed to disrupt the amount of water in the active site (Panels E, F, G, H. Figure 2). Ub-K129- and Ub-K488-MPO showed an increased amount of water molecules in the active site relative to the MPO, while Ub-K505MPO decreased the amount of water close to the HEME group. This observation could be relevant to the enzymatic activity, as the substrates are chloride ions and hydrogen peroxide, which could increase the amount of water in the active site.

NETs from SLE patients are enriched in ISG15. We found a differential ISG15 expression characterized by higher amounts of ISG15 in NETs from active SLE patients compared with healthy donors by Western blot. (SLE [0.29(0.16–0.52)] vs healthy control ([0.04(0.040–0.090)] $p = 0.0357$) (Panel A and B of Fig. 3).

NETs are an extracellular source of ISG15 and H2B is one of the targets in SLE

ISG15 was found both intra and extracellularly in the NETs of patients with SLE by confocal microscopy (Panel A Fig. 4), but not in the NETs of healthy controls (Panel B Fig. 4). Accordingly, we found increased expression of ISG15 in lupus NETs (both spontaneous and LPS-induced) compared to healthy controls (p = 0.0179) (Panel C, Fig. 4).

The colocalization analysis was performed in the area considered as a NET, by immunofluorescence for ISG15 and three potential substrates, H2B, HMGB1 or LL-37. We found that H2B showed the higher colocalization (r = 0.81) (Panel D Fig. 4). The highest colocalization between ISG15 and H2B was found in spontaneous NETs of patients with SLE followed by the colocalization in LPS induced NETs from SLE patients and as expected, the lowest was observed in NETs from healthy controls, with a significant difference between lupus NETs and healthy controls samples (0.75 [0.73–0.86] vs 0.21 [0.18–0.23] $p < 0.05$) (Panel E Fig. 4). No colocalization was found between ISG15 and HMGB1 or LL37 in NETs from either SLE patients or healthy donors samples (data not shown). By this method we can confirm that there is colocalization of ISG15 and H2B in NETs of patients with SLE, but not in healthy controls, suggesting H2B as one of the main targets of ISGylation in lupus patients as well as NETosis as another source of ISG15 in SLE.

Enriched ISG15 NETs from SLE patients induce IFNγ production from diverse cellular subsets. To address the functional impact of ISG15 on the NETs from lupus patients, the production of IFNγ in subsets of T lymphocytes ($CD4^+$ and $CD8^+$) and NK cells was evaluated by multiparametric flow cytometry. Higher IFNγ production was found in total PBMCs that were stimulated with NETs from lupus patients that previously had shown to be enriched by ISG15 (Panel B Fig. 5) compared to cells stimulated with NETs from healthy controls (Panel C Fig. 5) (%IFNγ 6.5[6.31–10.1] vs 3.5[1.7–5.1]) $p < 0.05$). Figure 5 shows a higher production of IFNγ by stimulating different subsets of PBMCs with ISG15 enriched NETs from SLE patients, compared with NETs of healthy donors, lacking such post-translational modification, including $CD4^+$ lymphocytes (Panel F Fig. 5), $CD8^+$ lymphocytes (Panel G Fig. 5), and NK $CD56^+$ lymphocytes (Panel H Fig. 5).

Discussion

In the present work, we demonstrated the presence of PTMs related to ubiquitin tag (total ubiquitin and ISG15), in NETs from SLE patients, and their impact in the reactivation, proliferation and polarization of $CD4^+$ cells of SLE patients and controls. Furthermore, to our knowledge this is the first report on the differential patterns of water molecules and conformational changes in residues near the catalytic site of MPO conjugated to ubiquitin. Interestingly, our data also suggest NETs as a source of ISG15 in SLE and

shows that H2B is a main target of this PTM and its functional role in regulating IFNγ secretion by T lymphocytes in SLE.

The trend towards increased proliferative responses of $CD4^+$ T lymphocytes from patients with SLE, as well as the polarization towards Th1 and Th17 subpopulations producing IFNγ or IL17A in the presence of components of NETs such as recombinant MPO and ubiquitylated MPO is consistent with a previous study in which $CD4^+$ and $CD8^+$ T lymphocytes from controls stimulated with supernatants of NETs induced in vitro, had higher levels of CD25, CD69, phosphorylation of ZAP70, secretion of IFNγ and IL17A; however, there was no increase in the percentage of proliferation with ethinyl deoxyuridine (EdU) (39). This difference in proliferation could be related to a differential threshold for activation and proliferation signals, which could be reached by the NET components and therefore able to induce the production of effector cytokines such as IFNγ and IL17A, but insufficient to fully activate T cell proliferation. In agreement to this, other studies have described proliferation of PBMCs from patients with vasculitis associated with anti-neutrophil cytoplasm antibody (ANCA) by increasing MPO concentrations to 10 µg/mL (7, 40), which corroborates the requirement for a high concentration of MPO for the regulation of proliferation in T lymphocytes. Furthermore, the ability to produce IFNγ by PBMCs from patients with ANCA vasculitis at the dose we used for the activation of dendritic cells (5 µg/mL), had been previously described by ELISA and this production was not carried out when using lower doses (0.5 µg / mL) (8). This is the first study addressing the biological effect of the ubiquitin tag in MPO in the context of systemic autoimmunity. Interestingly, the proliferative response of $CD4^+$ lymphocytes depends on the ubiquitin tag as well as the disease state (ie healthy controls vs SLE). It has been described that the type of response that is mounted (proinflammatory vs anti-inflammatory) is mainly related to the context in which the antigenic determinant (immunogen or tolerogen) is seen, highlighting the microenvironment, the PTMs and the disease state as key elements for the functional effect of every antigen (41). It is feasible that the relationship of ubiquitin with a lower activation and proliferation of $CD4^+$ T cells in controls is due to its ability to mask potentially dangerous antigens for the system (such as MPO in NETs) (42). Nonetheless, this relationship is in turn unbalanced in the context of SLE where both MPO with and without ubiquitin was able to induce polarization of $CD4^+$ T cells towards a Th1 and Th17 effector phenotype. This is in agreement with previous data from our research group suggesting that lupus patients have a ubiquitin deficiency state involving diverse cellular subsets and processes, in which they express lower amounts of E3 ligases (key enzymes for ubiquitylation) in T cells (43, 44) as well as diminished polyubiquitin K63 chains in NETs (11),, both with functional impact, such as resistance to anergy and altered macrophage responses, respectively. Accordingly, in healthy controls, the presence of ubiquitin tag involves a suppressive mechanism when it is bound to a molecule with a dual role in inflammatory signaling, such as MPO, which might be diminished in the context of systemic autoimmune diseases, such as SLE, explaining the shift towards Th1 and Th17 in $CD4^+$ cells in patients and the tolerogenic role in controls, diminishing the activation and proliferative responses.

The molecular dynamics simulations allowed to describe the closeness of arginine 239 (R239) when ubiquitin was bound to K505 or K488 compared to native MPO. R239 is an important residue of the

polypeptide chain lying near the distal face of the HEME group (45) and has been involved in the catalytic mechanism of MPO (46). There is evidence using molecular docking that the LGM2605 peptide, by its hydroxyl group, inhibits the enzymatic activity of MPO by blocking R239. The authors propose that while this position may not directly displace H_2O_2 binding, blocking the substrate channel may slow H_2O_2 access to HEME (47). Our results using contact map analysis allowed us to find that R239 decreased its distance from the HEME group when ubiquitin was conjugated to K505 or K488 compared to native MPO. This implies a lower probability of entry to the active site by the reaction substrates (Cl^- and H_2O_2).

One of the most relevant changes in the structural dynamics of the MPO was the differential hydration of the active site mediated by the ubiquitinated lysine residue. Water molecules are relevant to receptor-ligand recognition because they modify the geometry of the active site and contribute to binding affinity. Our results propose that when ubiquitin conjugates to K129 or K488, the number of water molecules close to the HEME group increases, and the opposite occurs when ubiquitin binds to K505. This differential pattern has been demonstrated in states of activation of receptors associated with G proteins where the role of water molecules is relevant to define the direction and magnitude of the movements of these proteins(48). It has been reported that in squid rhodopsin, the conformation of its active state is accompanied by an increase in the number of internal water molecules (IWM) and that inter-helix water molecules directly affect water-mediated interactions in the activation process (49). In a model of recognition of vasopressin and oxytocin receptors, it was found that very few water molecules interact with the D2.50 domain of the active site and appear to be a fundamental to stabilize their structure and participate in the binding of ligands (50), which could be similar to what was found in the MPO, highlighting the potential functional translation of the conformational changes related to the ubiquitin tag.

Furthermore, the evolution of structures is consistent with functional specificity, and ubiquitin-like proteins are an obvious example of the pleiotropism inherent in their function, as is the case with the 15 kDa IFN-related gene. ISG15 is another PTM that has a great diversity of functions depending on its location. Recently it has been identified the lymphocyte function-associated antigen 1 (LFA-1) or CD11a/αL as the putative receptor of ISG15 in NK cells inducing the activation of Src kinases and IFNγ and IL10 synthesis (51). However, currently, the release mechanism is unknown, secretory granules of neutrophils, lysosomes, exosomes, apoptotic bodies, and microvesicles released from infected macrophages have been suggested as probable mechanisms (52). Based on our results, we can propose a new non-canonical secretion mechanism of ISG15 by NETosis in patients with SLE. To our knowledge, this is the first report of extracellular ISG15 as a component of NETs only in SLE patients, highlighting its role in this disease. It is feasible to propose NETosis as one of the non-canonical secretion mechanisms of extracellular ISG15, since the increased levels of type I IFN, and the molecular transcriptional signature of SLE are suggested to be key pathogenic players in the disease. (13) (53)

In cells that respond to interferon, ISG15 as conjugated or free, the latter with "cytokine-like" activity with evidence supporting its ability to induce the production of IFNγ as well (54, 55). Additionally, controversy exists about the pathogenic role of ISG15, since the overexpression of ISG15 in NETs of SLE patients

could be both a consequence of the overstimulation by the IFNα/β signature, and a signal from NETs involved in the production of IFNγ by lymphocyte subpopulations (56, 57). Our data show that indeed NETs from SLE patients are capable of inducing IFNγ production in $CD4^+$ T lymphocytes as has been previously shown by Tillack KB, *et al* (39).

Finally, we show that the protein cargo of NETs from SLE patients is enriched in ISG15 and able to induce IFNγ production, which agrees with previous data by Iglesias-Guimarais, et al (58) which show that in addition to $CD4^+$ lymphocytes, IFNγ production was also reported by other subpopulations such as $CD8^+$ and NK cells, both known targets of action of extracellular ISG15 (58), which is also produced by lupus plasma cells (57). Therefore, it can be argued that NETs promote the activation of these cells with the subsequent production of IFNγ in response (among other stimuli) to free ISG15. (59, 60) Thus, we propose ISG15 in NETs as a new component in the physiopathogenic scheme of autoimmune diseases such as SLE, with an effector correlate that includes the induction of Th1 lymphocytes with a proinflammatory potential (Fig. 6. Graphical abstract). There is evidence that the deficiency of ISG15, through the ISGylation of USP18, can degrade this potent inhibitor of IFNα/β-mediated signaling and promote its accumulation (12), therefore ISG15 has even been proposed as a downregulator of type 1 IFN (59), and may have a different functional profile depending on its binding to ISGylated substrates or its extracellular release, as shown in the present study and previous reports in which the administration of free ISG15 as an adjuvant, helps to enhance the production of IFNγ and an increase in the cytolytic activity of $CD8^+$ T cells against papillomavirus (61).

More than 30% of the ISG15 targets were described by mass spectrometry as nuclear proteins (56). These data suggest histones (nuclear proteins that are part of NETs) as potential targets for this PTM (62, 63). The ubiquitin label in H2B (K123) has been found to affect chromatin dynamics and RNA polymerase passage to facilitate a robust transcription system (64), (65). So far, this has been the closest evidence that ubiquitin or some other ubiquitin-like protein is related to histone conjugation, specifically H2B. Therefore, we propose H2B as a candidate substrate for ISG15, whose conjugation might induce changes in structure and function as previously reported with other PTMs in chromatin, and a source of autoantigens in autoimmune pathologies (63).

Our study has many limitations. First, it is a transversal study with no tracing of patient's characteristics. Also, we used effector $CD4^+$ in the cocultures with DC, instead of naïve $CD4^+$, resulting in a reactivation profile of *ex vivo* Th1 or Th17 instead of *in vitro* Th0 polarization. Nevertheless, it is the first study to address the *in vitro, in silico* and *ex vivo* role of ubiquitin and NETosis-released-ISG15, their impact on cellular responses from SLE patients as well as the improvement in our knowledge of the pathophysiology of Lupus and autoimmunity.

Conclusions

In summary, UbMPO can induce the reactivation of Th1 and Th17 cells, producing IFNγ and IL17A; enhanced proliferation in SLE patients, as well as dampened activation and proliferation in healthy

donors T cells, highlighting the presence of changes in the intrinsic dynamics of MPO when conjugated with ubiquitin. Besides, our data suggest that NETosis is a non-canonical release mechanism for ISG15, suggest H2B as a specific substrate for ISG15 in SLE patients and these ISG15 enriched NETs from SLE patients promote enhanced production of IFNγ, implying a new field in pleiotropic functions of PTM promoting tolerogenic and immunogenic responses during autoimmune diseases.

Abbreviations

ACR
American College of Rheumatology
ANCA
antineutrophil cytoplasmic antibodies
CHARMM
Chemistry at HARvard Macromolecular Mechanics
Cl^-
chloride
DC
dendritic cells
dsDNA
double stranded deoxyribonucleic acid
ECL
enhanced chemiluminescence
EdU
ethinyl deoxyuridine
ELISA
Enzyme-Linked Immunosorbent Assay
FBS
fetal bovine serum
FoxP3
forkhead box protein P3
GM-CSF
Granulocyte Macrophage Colony-Stimulating Factor
H2B
histone 2 B
H_2O_2
hydrogen peroxide
HEPES
4-(2-hydroxyethyl)-1-piperazineethanesulfonic acid
HMGB1
High mobility group box 1 protein

HRP
horseradish peroxidase
IFN
Interferon
IIWM
internal water molecules
IQR
interquartile range
ISG15
Interferon-stimulated gene 15
K129-MPO
lysine129 of myeloperoxidase
K488-MPO
lysine488 of myeloperoxidase
K505-MPO
lysine505 of myeloperoxidase
LFA-1
lymphocyte function-associated antigen 1
LGM2605
Synthetic Secoisolariciresinol Diglucoside
LL37
cathelicidin antimicrobial peptide 18
LPS
lipopolysaccharide
MACS
magnetic cell separation
MoDCs
monocyte derived dendritic cells
MPO
myeloperoxidase
NaCl
sodium chloride
NAMD
Nanoscale Molecular Dynamics
NE
neutrophil elastase
NETs
neutrophil extracellular traps
PBMCs
peripheral blood mononuclear cells

PBS
phosphate buffered saline
PDB
protein data bank
PMA
phorbol 12-myristate 13-acetate
PTM
post-translational modification
PVDF
polyvinylidene fluoride
R239
arginine 239
rhMPO
recombinant human MPO
RMSD
root-mean-square deviation
RNA
ribonucleic acid
ROS
reactive oxygen species
RPMI
Roswell Park Memorial Institute
SASA
solvent-accessible surface area
SLE
Systemic lupus erythematosus
SLEDAI
Systemic Lupus Erythematosus Disease Activity Index
TBS
tris-buffered saline
TNF-α
tumor necrosis factor alpha
UbMPO
ubiquitylated MPO
USP18
Ubiquitin Specific Peptidase 18
VMD
Visual Molecular Dynamics
ZAP70
Zeta Chain Of T Cell Receptor Associated Protein Kinase 70

Declarations

Ethics approval and consent to participate:

All healthy controls and SLE patients signed an informed consent before inclusion, and the protocol was approved by our Institutional Ethics Committee (Ref. 2152) in compliance with the Helsinki declaration.

Consent for publication:

The images and data contained in this manuscript are not related to a single individual and are entirely unidentifiable.

Availability of data and materials:

The datasets used and/or analyzed during the current study are available from the corresponding author on reasonable request.

Competing interests:

The authors declare that they have no competing interests

Conflict of Interest:

The authors declare they have no competing financial interests.

Funding:

This study was supported by a grant from the Consejo Nacional de Ciencia y Tecnología (CONACYT, 255941, SEP-Ciencia Básica 2015).

Author contributions:

DG participated in the conceptualization, design, investigation process, project administration, supervision, formal analysis, validation, and critical revision of the manuscript. DC and EJ participated in the investigation process, data curation, formal analysis, validation and visualization of the work, and writing the original draft. JA participated in the conceptualization and critical revision of the manuscript. JT, JM, DM, GJ, MD participated in the investigation process and data curation. All authors read and approved the final manuscript.

Acknowledgements:

We would like to thank the technical support provided by the Red de Apoyo a la Investigación CIC-UNAM. The figures were done using icons taken from BioRender App in https://biorender.com/.

References

References:

1. Papayannopoulos V. Neutrophil extracellular traps in immunity and disease. Nat Rev Immunol. 2018;18(2):134–47.
2. Brinkmann V, Reichard U, Goosmann C, Fauler B, Uhlemann Y, Weiss DS, et al. Neutrophil extracellular traps kill bacteria. Science. 2004;303(5663):1532–5.
3. Goel RR, Kaplan MJ. Deadliest catch: neutrophil extracellular traps in autoimmunity. Curr Opin Rheumatol. 2020;32(1):64–70.
4. Petretto A, Bruschi M, Pratesi F, Croia C, Candiano G, Ghiggeri G, et al. Neutrophil extracellular traps (NET) induced by different stimuli: A comparative proteomic analysis. PLoS One. 2019;14(7):e0218946.
5. Papayannopoulos V, Metzler KD, Hakkim A, Zychlinsky A. Neutrophil elastase and myeloperoxidase regulate the formation of neutrophil extracellular traps. J Cell Biol. 2010;191(3):677–91.
6. Odobasic D, Kitching AR, Yang Y, O'Sullivan KM, Muljadi RC, Edgtton KL, et al. Neutrophil myeloperoxidase regulates T-cell-driven tissue inflammation in mice by inhibiting dendritic cell function. Blood. 2013;121(20):4195–204.
7. Griffith ME, Coulthart A, Pusey CD. T cell responses to myeloperoxidase (MPO) and proteinase 3 (PR3) in patients with systemic vasculitis. Clin Exp Immunol. 1996;103(2):253–8.
8. Popa ER, Franssen CF, Limburg PC, Huitema MG, Kallenberg CG, Tervaert JW. In vitro cytokine production and proliferation of T cells from patients with anti-proteinase 3- and antimyeloperoxidase-associated vasculitis, in response to proteinase 3 and myeloperoxidase. Arthritis rheumatism. 2002;46(7):1894–904.
9. Knight JS, Zhao W, Luo W, Subramanian V, O'Dell AA, Yalavarthi S, et al. Peptidylarginine deiminase inhibition is immunomodulatory and vasculoprotective in murine lupus. J Clin Invest. 2013;123(7):2981–93.
10. Pieterse E, Hofstra J, Berden J, Herrmann M, Dieker J, van der Vlag J. Acetylated histones contribute to the immunostimulatory potential of neutrophil extracellular traps in systemic lupus erythematosus. Clin Exp Immunol. 2015;179(1):68–74.
11. Barrera-Vargas A, Gomez-Martin D, Carmona-Rivera C, Merayo-Chalico J, Torres-Ruiz J, Manna Z, et al. Differential ubiquitination in NETs regulates macrophage responses in systemic lupus erythematosus. Ann Rheum Dis. 2018;77(6):944–50.
12. Zhang X, Bogunovic D, Payelle-Brogard B, Francois-Newton V, Speer SD, Yuan C, et al. Human intracellular ISG15 prevents interferon-alpha/beta over-amplification and auto-inflammation. Nature.

2015;517(7532):89–93.
13. Chasset F, Arnaud L. Targeting interferons and their pathways in systemic lupus erythematosus. Autoimmun rev. 2018;17(1):44–52.
14. Hochberg MC. Updating the American College of Rheumatology revised criteria for the classification of systemic lupus erythematosus. Arthritis rheumatism. 1997;40(9):1725.
15. Posch W, Lass-Florl C, Wilflingseder D. Generation of Human Monocyte-derived Dendritic Cells from Whole Blood. J Vis Exp. 2016(118).
16. Dauer M, Obermaier B, Herten J, Haerle C, Pohl K, Rothenfusser S, et al. Mature dendritic cells derived from human monocytes within 48 hours: a novel strategy for dendritic cell differentiation from blood precursors. J Immunol. 2003;170(8):4069–76.
17. Fiedler TJ, Davey CA, Fenna RE. X-ray crystal structure and characterization of halide-binding sites of human myeloperoxidase at 1.8 Å resolution. J Biol Chem. 2000;275(16):11964–71.
18. Vijay-Kumar S, Bugg CE, Cook WJ. Structure of ubiquitin refined at 1.8Åresolution. J Mol Biol. 1987;194(3):531–44.
19. Humphrey W, Dalke W, Schulten K. VMD: Visual molecular dynamics. JMolGraphics. 1996;14(1):33–8.
20. Phillips JC, Braun B, Wang W, Gumbart J, Tajkhorshid E, Villa E, et al. Scalable molecular dynamics with NAMD. J Comput Chem. 2005;26:1781–802.
21. Martyna GJ, Tobias DJ, Klein ML. Constant-pressure molecular-dynamics algorithms. JChemPhys. 1994;101:4177–89.
22. Feller SE, Zhang Y, Pastor RW, Brooks BR. Constant pressure molecular dynamics simulation: The Langevin piston method. JChemPhys. 1995;103(11):4613–21.
23. Grubmüller H, Heller H, Windemuth A, Schulten K. Generalized Verlet algorithm for efficient molecular dynamics simulations with long-range interactions. Mol Simul. 1991;6:121–42.
24. Tuckerman M, Berne BJ. Reversible multiple time scale molecular dynamics. JChemPhys. 1992;97(3):1990–2001.
25. Darden T, York D, Pedersen L. Particle mesh Ewald: An *N*•log(*N*) method for Ewald sums in large systems. JChemPhys. 1993;98:10089–92.
26. Essmann U, Perera L, Berkowitz ML, Darden T, Lee H, Pedersen LG. A smooth particle mesh Ewald method. JChemPhys. 1995;103:8577–93.
27. Miyamoto S, Kollman P. An analytical version of the SHAKE and RATTLE algorithm for rigid water models. J Comput Chem. 1992;13:952–62.
28. Best RB, Zhu X, Shim J, Lopes PEM, Mittal J, Feig M, et al. Optimization of the additive CHARMM all-atom protein force field targeting improved sampling of the backbone phi, psi and side-chain chi1 and chi2 dihedral angles. J Chem Theory Comput. 2012;8:3257–73.
29. MacKerell AD Jr, Bashford D, Bellott M, Dunbrack RL Jr, Evanseck JD, Field MJ, et al. All-atom empirical potential for molecular modeling and dynamics studies of proteins. JPhysChemB.

1998;102(18):3586–616.

30. MacKerell AD Jr, Feig M, Brooks CL. II. Extending the treatment of backbone energetics in protein force fields: Limitations of gas-phase quantum mechanics in reproducing conformational distributions in molecular dynamics simulations. JComputChem. 2004;25:1400–15.
31. MacKerell AD, Feig M, Brooks CL. Improved Treatment of the Protein Backbone in Empirical Force Fields. J Am Chem Soc. 2004;126(3):698–9.
32. Jorgensen WL, Chandrasekhar J, Madura JD, Impey RW, Klein ML. Comparison of simple potential functions for simulating liquid water. JChemPhys. 1983;79(2):926–35.
33. Carmona-Rivera C, Kaplan MJ. Detection of SLE antigens in neutrophil extracellular traps (NETs). Methods Mol Biol. 2014;1134:151–61.
34. Carmona-Rivera C, Kaplan MJ. Induction and Quantification of NETosis. Curr Protoc Immunol. 2016;115:14 41 1–14 41 14.
35. Costes SV, Daelemans D, Cho EH, Dobbin Z, Pavlakis G, Lockett S. Automatic and quantitative measurement of protein-protein colocalization in live cells. Biophys J. 2004;86(6):3993–4003.
36. Ratner B. The correlation coefficient: Its values range between + 1/–1, or do they? Journal of Targeting Measurement Analysis for Marketing. 2009;17(2):139–42.
37. Bombardier C, Gladman DD, Urowitz MB, Caron D, Chang CH. Derivation of the SLEDAI. A disease activity index for lupus patients. The Committee on Prognosis Studies in SLE. Arthritis rheumatism. 1992;35(6):630–40.
38. Carpena X, Vidossich P, Schroettner K, Calisto BM, Banerjee S, Stampler J, et al. Essential role of proximal histidine-asparagine interaction in mammalian peroxidases. J Biol Chem. 2009;284(38):25929–37.
39. Tillack KB, Martin P, Sospedera R. M. T Lymphocyte Priming by Neutrophil Extracellular Traps Links Innate and Adaptive Immune Responses. J Immunol. 2012;188(7):3150–9.
40. King WJ, Brooks CJ, Holder R, Hughes P, Adu D, Savage CO. T lymphocyte responses to anti-neutrophil cytoplasmic autoantibody (ANCA) antigens are present in patients with ANCA-associated systemic vasculitis and persist during disease remission. Clin Exp Immunol. 1998;112(3):539–46.
41. Matzinger P. The danger model: a renewed sense of self. Science. 2002;296(5566):301–5.
42. Weil R. Does antigen masking by ubiquitin chains protect from the development of autoimmune diseases? Front Immunol. 2014;5:262.
43. Gómez-Martín D, Ibarra-Sánchez M, Romo-Tena J, Cruz-Ruíz J, Esparza-López J, Galindo-Campos M, et al. Casitas B lineage lymphoma b is a key regulator of peripheral tolerance in systemic lupus erythematosus. Arthritis rheumatism. 2013;65(4):1032–42.
44. Gómez-Martín D, Díaz-Zamudio M, Alcocer-Varela J. Ubiquitination system and autoimmunity: the bridge towards the modulation of the immune response. Autoimmun rev. 2008;7(4):284–90.
45. Babior BM. Reactive Oxygen Species in Biological Systems: An Interdisciplinary Approach. The Production and Use of Reactive Oxidants by Phagocytes: Springer Science & Business Media.; 2007.

46. Zeng J, Fenna RE. X-ray crystal structure of canine myeloperoxidase at 3 Å resolution. Journal of molecular biology. 1992;226(1):185–207.
47. Mishra OP, Popov AV, Pietrofesa RA, Nakamaru-Ogiso E, Andrake M, Christofidou-Solomidou M. Synthetic secoisolariciresinol diglucoside (LGM2605) inhibits myeloperoxidase activity in inflammatory cells. Biochim Biophys Acta Gen Subj. 2018;1862(6):1364–75.
48. Jardón-Valadez E, Bondar A-N, Tobias DJ. Dynamics of the internal water molecules in squid rhodopsin. Biophysical journal. 2009;96(7):2572–6.
49. Grossfield A, Pitman MC, Feller SE, Soubias O, Gawrisch K. Internal hydration increases during activation of the G-protein-coupled receptor rhodopsin. Journal of molecular biology. 2008;381(2):478–86.
50. Ślusarz M, Slusarz R, Ciarkowski J. Molecular Dynamics Study of the Internal Water Molecules in Vasopressin and Oxytocin Receptors. Protein Pept Lett. 2009;16:342–50.
51. Swaim CD, Scott AF, Canadeo LA, Huibregtse JM. Extracellular ISG15 Signals Cytokine Secretion through the LFA-1 Integrin Receptor. Molecular cell. 2017;68(3):581 – 90.e5.
52. Villarroya-Beltri C, Baixauli F, Mittelbrunn M, Fernández-Delgado I, Torralba D, Moreno-Gonzalo O, et al. ISGylation controls exosome secretion by promoting lysosomal degradation of MVB proteins. Nat Commun. 2016;7(1):13588.
53. Banchereau R, Hong S, Cantarel B, Baldwin N, Baisch J, Edens M, et al. Personalized Immunomonitoring Uncovers Molecular Networks that Stratify Lupus Patients. Cell. 2016;165(3):551–65.
54. D'Cunha J, Knight E Jr, Haas AL, Truitt RL, Borden EC. Immunoregulatory properties of ISG15, an interferon-induced cytokine. Proc Natl Acad Sci USA. 1996;93(1):211–5.
55. Bogunovic D, Byun M, Durfee LA, Abhyankar A, Sanal O, Mansouri D, et al. Mycobacterial disease and impaired IFN-γ immunity in humans with inherited ISG15 deficiency. Science (New York). 2012;337(6102):pp. 1684–8.
56. Zhao C, Denison C, Huibregtse JM, Gygi S, Krug RM. Human ISG15 conjugation targets both IFN-induced and constitutively expressed proteins functioning in diverse cellular pathways. 2005;102(29):10200–5.
57. Care MA, Stephenson SJ, Barnes NA, Fan I, Zougman A, El-Sherbiny YM, et al. Network Analysis Identifies Proinflammatory Plasma Cell Polarization for Secretion of ISG15 in Human Autoimmunity. J Immunol. 2016;197(4):1447–59.
58. Iglesias-Guimarais V, Ahrends T, de Vries E, Knobeloch K-P, Volkov A, Borst J. IFN-Stimulated Gene 15 Is an Alarmin that Boosts the CTL Response via an Innate, NK Cell-Dependent Route. J Immunol. 2020;204(8):2110–21.
59. Dos Santos PF, Mansur DS. Beyond ISGlylation: Functions of Free Intracellular and Extracellular ISG15. Journal of interferon cytokine research: the official journal of the International Society for Interferon Cytokine Research. 2017;37(6):246–53.
60. Hermann M, Bogunovic D. ISG15. In Sickness and in Health. Trends Immunol. 2017;38(2):79–93.

61. Villarreal DO, Wise MC, Siefert RJ, Yan J, Wood LM, Weiner DB. Ubiquitin-like Molecule ISG15 Acts as an Immune Adjuvant to Enhance Antigen-specific CD8 T-cell Tumor Immunity. Molecular therapy: the journal of the American Society of Gene Therapy. 2015;23(10):1653–62.
62. Neeli I, Khan SN, Radic M. Histone Deimination As a Response to Inflammatory Stimuli in Neutrophils. 2008;180(3):1895–902.
63. Bowman GD, Poirier MG. Post-translational modifications of histones that influence nucleosome dynamics. Chemical reviews. 2015;115(6):2274–95.
64. Pavri R, Zhu B, Li G, Trojer P, Mandal S, Shilatifard A, et al. Histone H2B Monoubiquitination Functions Cooperatively with FACT to Regulate Elongation by RNA Polymerase II. Cell. 2006;125(4):703–17.
65. Fleming AB, Kao C-F, Hillyer C, Pikaart M, Osley MA. H2B Ubiquitylation Plays a Role in Nucleosome Dynamics during Transcription Elongation. Molecular cell. 2008;31(1):57–66.

Figures

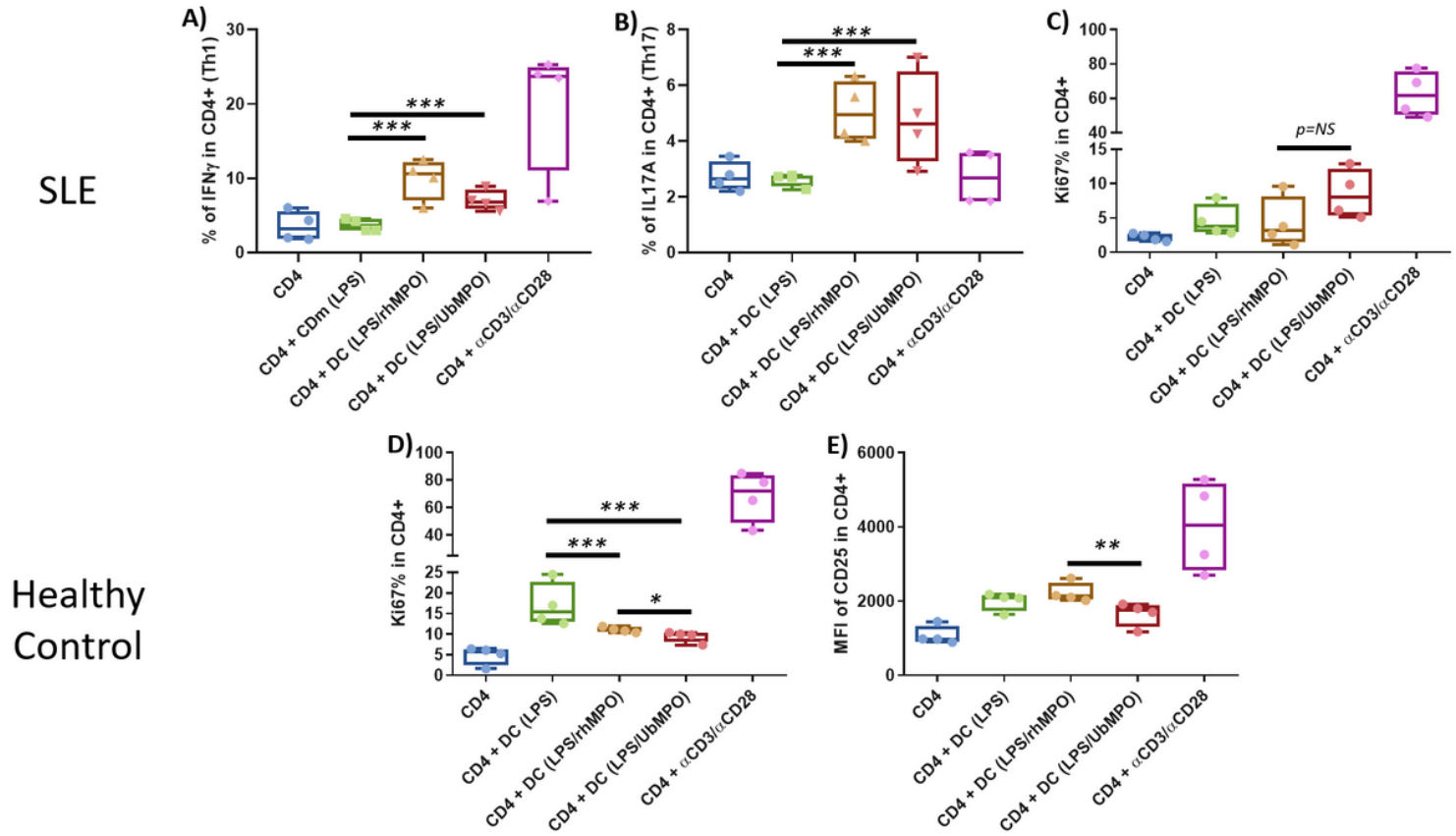

Figure 1

UbMPO regulates CD4+ lymphocyte activation, proliferation and cytokine production. CD4+ lymphocytes from SLE patients or healthy controls were cocultured with LPS activated DCs with UbMPO or rhMPO. Increased production of proinflammatory cytokines, IFNγ (A) and IL17A (B) was documented for CD4+ lymphocytes from SLE patients upon stimulation with UbMPO. A differential proliferative response was

found between SLE and healthy controls, with increased proliferation from the lupus samples (C) and decreased proliferation from healthy controls (D) towards UbMPO stimulation. Lower activation of healthy control CD4+ lymphocytes upon UbMPO stimulation was found (E). * p=0.0421. **p=0.03038. ***p=0.0286.

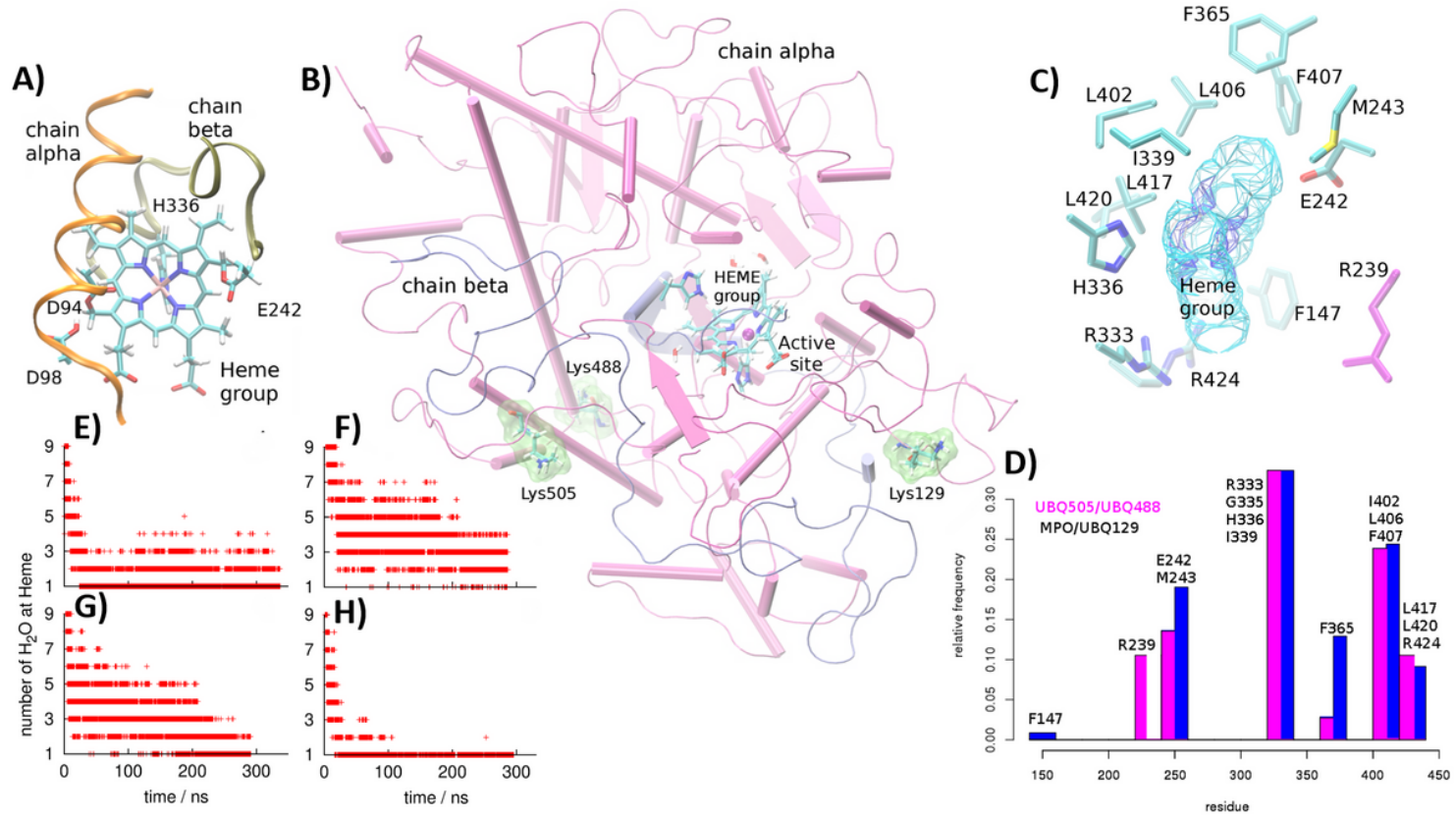

Figure 2

Molecular Dynamics simulations. MPO active site and ubiquitylation sites. Close-up of the HEME group in the native MPO active site showing ester bonds of the D94, E292 side chains and the methyls at position 3 and 13 of the HEME group (A). Representation in licorice. Fragments of chain and chain are shown in orange and ochre ribbons as context of the active site, as well as H. Structure of the native MPO in cartoons representation (B), chain a in magenta and chain b in ice blue. In licorice representation the HEME group, axial histidine, lysines 129, 488 and 505, and three water molecules in the active site. Color code: Color code C, cyan, O, red, H, white N, blue, Fe, pink. Visual representation of the residues near the HEME group. R239 was found close to the active site only when ubiquitin was conjugated to K505 or K488 (C). Contact map of the residues of the MPO in close contact with the HEME group, highlights the differential profile when the ubiquitin is found in K505 or K488 over R239 (D). Number of water molecules in the active site as a function of simulation time. In the crystal structure, there are 3.5 water molecules in this region of the protein. Compared to the native MPO (E), ubiquitylation at K129 (F) or K488 (G) the number of water molecules increases by 1 to 3 molecules; in K505 (H) the amount of water in the active decreases up to 1. The hydration level at the active site was sensitive to the ubiquitylation site.

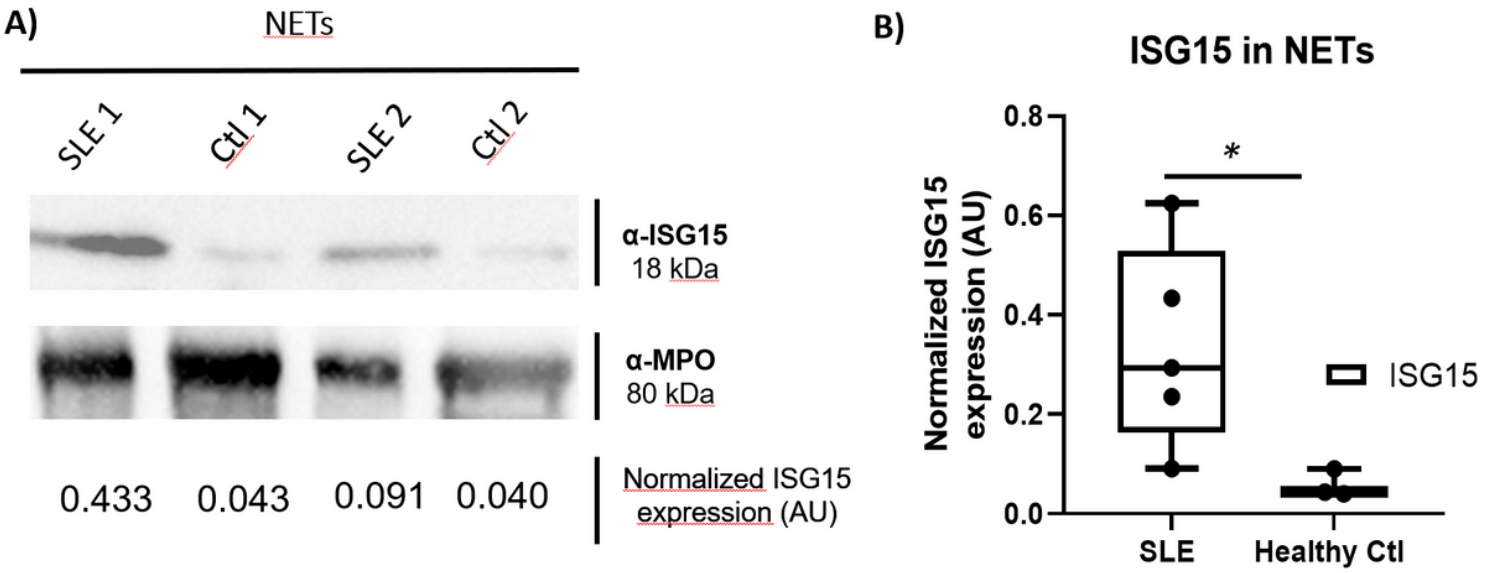

Figure 3

NETs from SLE patients are enriched in ISG15. Western Blot analysis of LPS induced NETs from SLE patients and healthy controls (n=2 subjects per group) was performed and quantification was done by densitometry. MPO was used as a loading control. Representative blots for ISG15 expression are included (A) and increased expression of ISG15 in NETs from SLE patients (n=5) vs healthy controls (n=3) is shown in B. *p=0.0357.

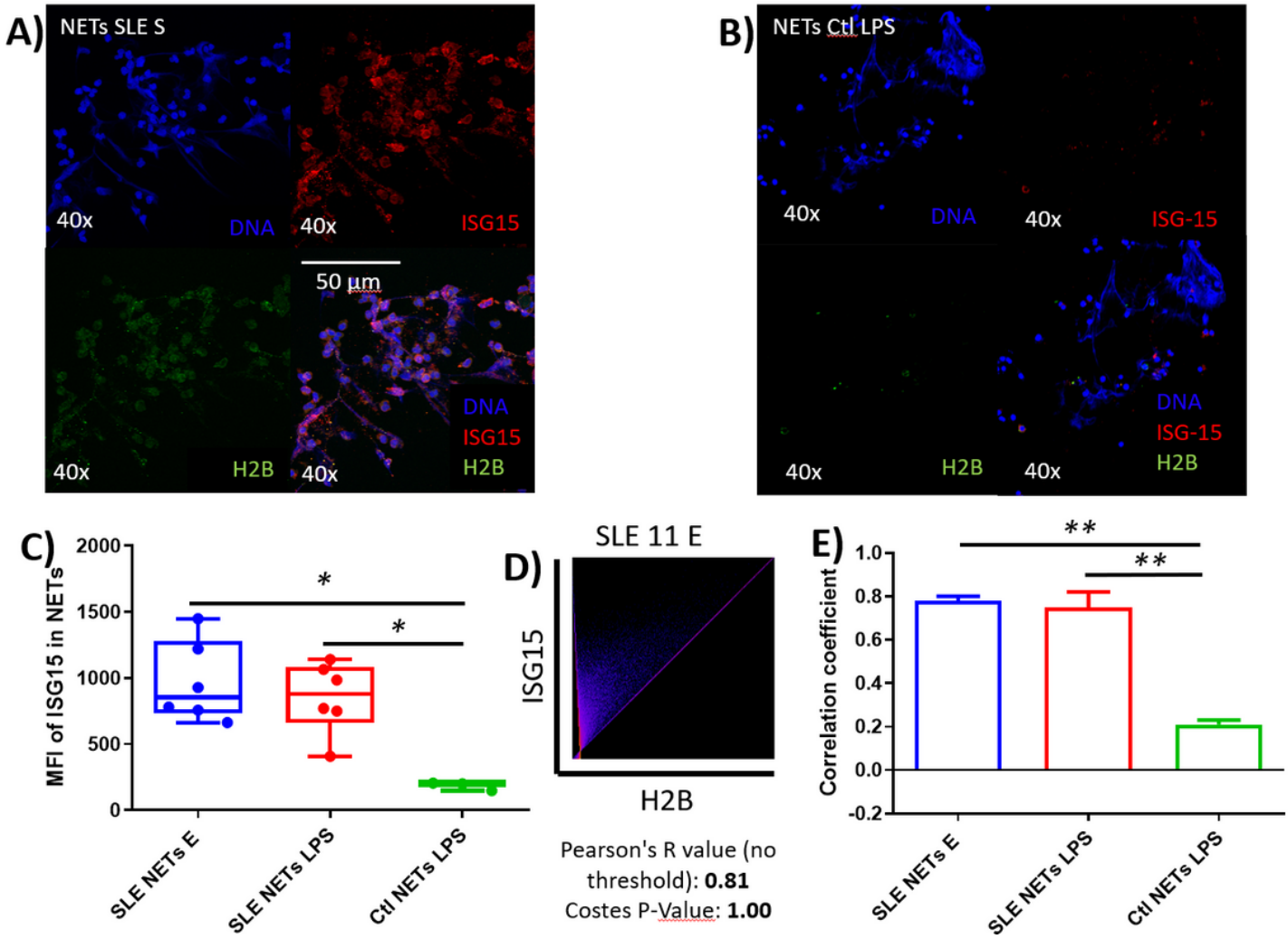

Figure 4

NETs from SLE patients are enriched in ISG15 and H2B is the main substrate. ISG15 and H2B expression was assessed in spontaneous and LPS induced NETs from SLE patients (n=6) and healthy controls (n=3) by indirect immunofluorescence (40X) and confocal microscopy. Spontaneous NETs from a representative SLE patient shows the presence of extracellular ISG15 in the NET (A). In contrast to the SLE sample, a representative healthy control image shows the absence of ISG15 in the NET (B). Blue (DNA), red (ISG15) and green (H2B). Pooled data from SLE patients and healthy controls (n=6 subjects per group) show increased expression of ISG15 in the SLE samples (C). In SLE samples, ISG15 and H2B colocalized inside NETs with a high Pearson (R= 0.81) and Costes p value (1.0) in a representative SLE patient and boxes represent pooled data (n=6 subjects per group) that show increased colocalization of SLE samples vs healthy controls (E). * p=0.0179; ** p<0.05

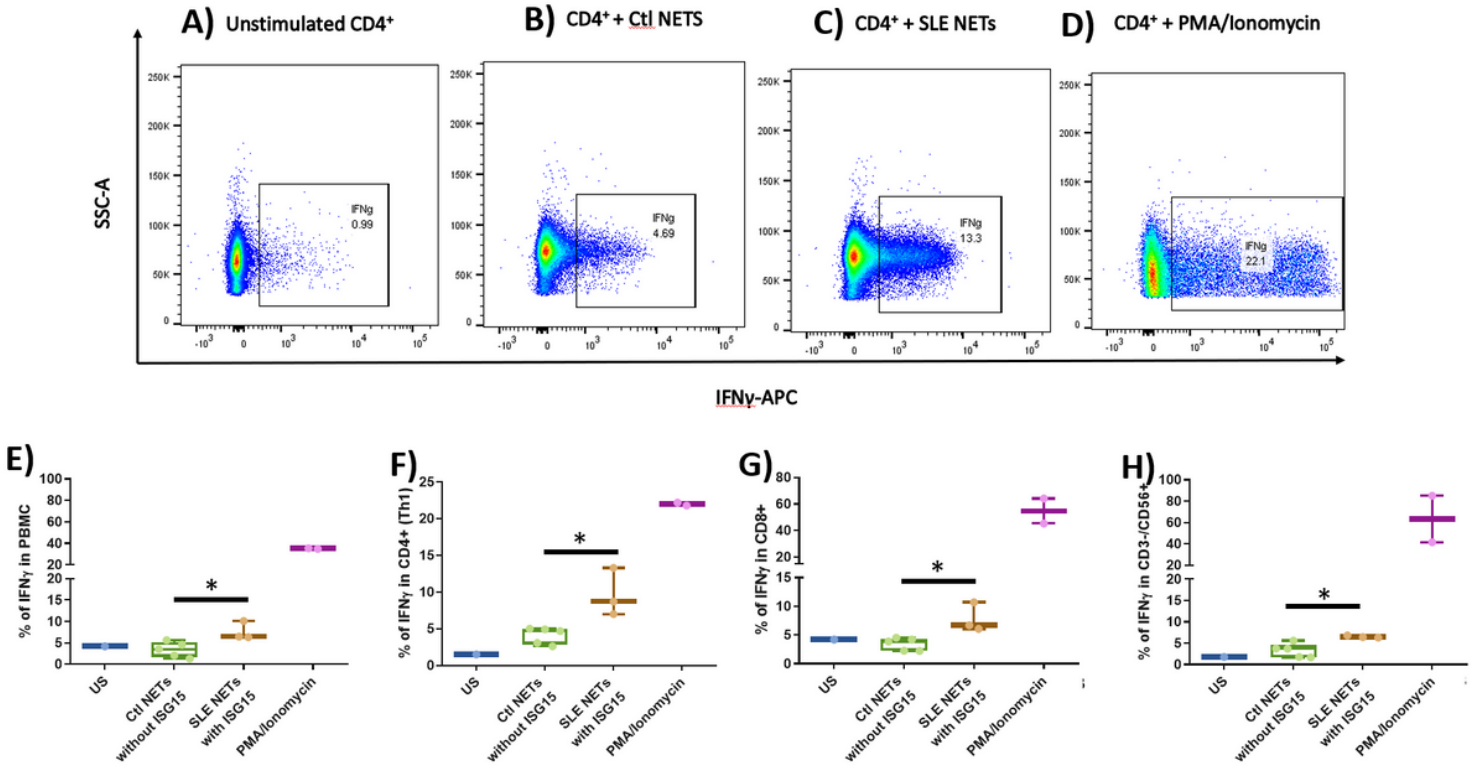

Figure 5

NETs enriched in ISG15 promote the production of IFNγ in different PBMCs subsets. IFNγ+ cells from different PBMCs subsets from healthy controls were assessed by flow cytometry under different experimental conditions. A representative dot plot from one healthy control is shown for each experimental condition as follows: A) Unstimulated; B) NETs from healthy controls without ISG15 expression; C) NETs from SLE patients enriched in ISG15; D) PMA+Ionomycin. Boxes (median ± interquartile range) represent the pooled data from healthy controls (n=3) and show increased expression of IFNγ+ cells when total PBMCs (E), CD4+ lymphocytes (F), CD8+ lymphocytes (G) and NK cells (H) were stimulated with SLE NETs enriched in ISG15. * p=0.0357

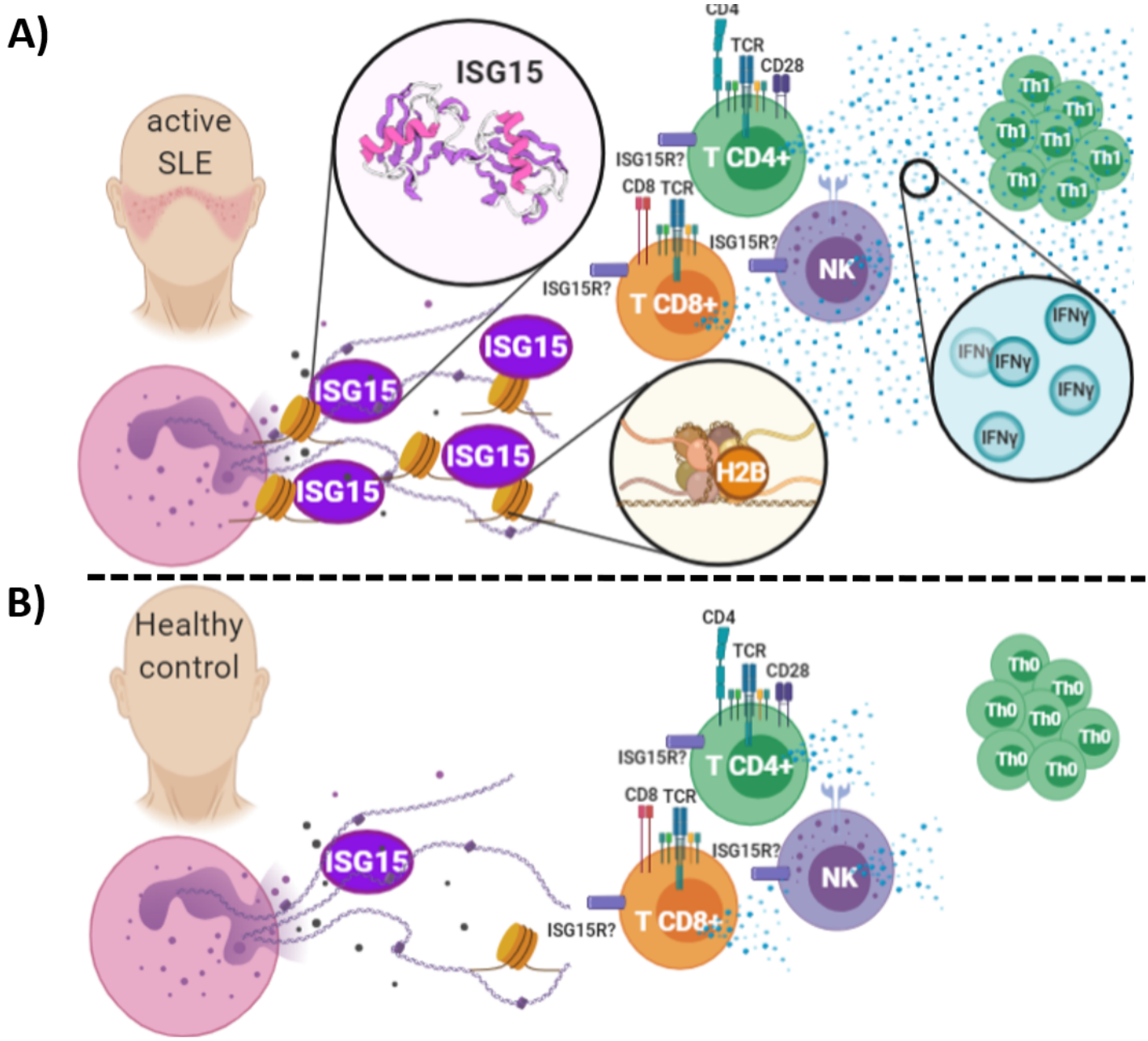

Figure 6

Graphical abstract: NETosis as a non-canonical release mechanism of ISG15 in SLE. In lupus patients, the NETs protein cargo is consistent with augmented amount of ISG15, which colocalized with H2B and induce the activation of CD4+, CD8+ and NK to a Th1 subset that enhanced the production of IFNγ (A). Low concentrations of ISG15 were found in healthy controls NETs with a diminished colocalization with H2B and reduction of IFNγ production by CD4+, CD8+ and NK cells (B). Therefore, ISG15 is a fingerprint of the interferogenic signature, and its release is mediated through NETosis in lupus patients.

Supplementary Files

This is a list of supplementary files associated with this preprint. Click to download.

- FigureSupplementaryPTMNETSLE.pptx